Webcam based in-vacuum tomography of plasma thruster jets

Mick Wijnen[1,*], **Jaume Navarro-Cavallé**[1], **Yacine Babou**[1], **Pablo Fajardo**[1]

[1]Equipo de Propulsión Espacial y Plasmas (EP2), Universidad Carlos III de Madrid, Leganés, Spain
*corresponding author: mwijnen@pa.uc3m.es

Abstract Diagnostics of plasma plumes are indispensable for both characterizing thruster performance and investigating the underlying physics of new thruster technologies. Most existing diagnostics either provide local or line-of-sight information and often require the assumption of axi-symmetry. Tomography does not have these limitations. By combining images taken at different viewing angles the 3D distribution of light intensity can be reconstructed. By the judicious use of spectral filters and a collisional- radiative model the light intensity can be related to electron temperature and plasma density. In this preliminary work we present a low-cost tomography experimental setup based on commercially available webcams which are shown to operate inside the vacuum environment. Some preliminary results are analyzed to showcase the potential of this diagnostic method.

1 Introduction

Most plasma diagnostics for thruster plumes are perturbing, i.e. affect the flow, and provide only local or line-of-sight measurements. Tomography can be used to overcome these limitations, it is non-perturbing and can provide a 3D reconstruction of the plasma emission from which certain plasma parameters can be derived. Although this technique is not entirely new [1][2], in this work we present and evaluate the preliminary characteristics of a low-cost setup based on commercially available webcams operated inside a vacuum environment.

2 Tomography

Tomography is a technique that reconstructs 3D distributions based on 2D projections. Consider a 2D plasma with a light intensity distribution $J(x,y)$ centered on O. Consider also a rotated reference frame (x',y'), rotated by an angle θ. A line-of-sight intensity profile $I(\theta,x')$ can now be constructed on a line at a viewing distance $y'=d$ and along the x' direction. A sketch of the problem can be seen in figure 1. Knowing the distribution $J(x,y)$, the distribution $I(\theta,x')$ at any viewing angle θ can be found from the Radon transform. Inversely the distribution $J(x,y)$ can be constructed from a (limited) number of projected profiles $I(\theta,x')$ at different viewing angles using the inverse Radon transform [3].

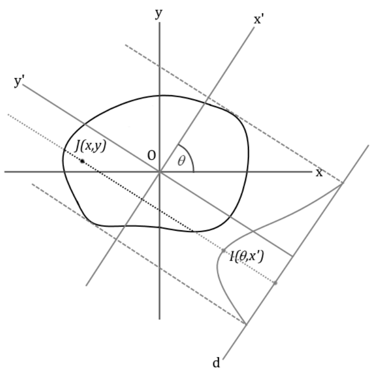

Fig. 1 Tomographic principle.

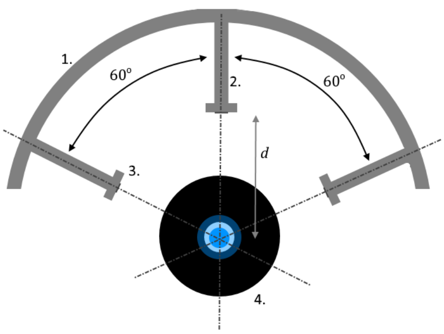

Fig. 2 Schematic of the setup. 1) arc; 2) extension; 3) webcam; 4) coil.

This can easily be extend to a 3D situation for a distribution $J(x,y,z)$ where $I(\theta,x',z)$ are projections at different z (axial) positions. In practice the projections $I(\theta,x',z)$ are obtained at discrete values θ_k and x'_i and z_j where the latter two correspond to the pixels (row and columns) of the CMOS array.

For optically thin plasmas (as is the case for thruster plumes) the line-of-sight intensity at a viewing angle θ and $\theta+\pi$ are the same reducing the useful domain to $[0,\pi]$. Within this domain K equally spaced planes at angles θ_k are obtained. More distinct viewing angles capture more information about the distribution $J(x,y)$, however, generally K is limited in the set-up. In our case, the limitations comes by the number of cameras where $K = 3$. To overcome this limitation we make use of trigonometric interpolation where we adopt the method of [1].

For each value of z, i.e. one line of the pixel array, the measured intensity profiles $I(\theta_k,x)$ (where we dropped the prime for convenience) are interpolated using a polynomial of order N:

$$I(\theta_k,x) = \sum_{n}^{N} c_n(\theta_k)x^n \tag{1}$$

N has to be large enough to have an adequate fitting of the line-of-sight intensity profile, $I(\theta,x)$. In this work a value of $N = 24$ is used. Then, using trigonometric interpolation we can then find coefficients $c_n(\theta)$ for any viewing angle θ.

$$c_n(\theta) = \frac{1}{2}a_{n0} + \sum_{m=1}^{K-1}(a_{nm}\cos m\theta + b_{nm}\sin m\theta) + \frac{1}{2}a_{nK}\cos K\theta \tag{2}$$

The coefficients a_{nm} and b_{nm} are given by:

$$a_{nm} = \frac{2}{K}\sum_{k=1}^{K} c_n(\theta_k)\cos m\theta_k \quad \text{if} \quad n+m \quad \text{is even, otherwise} \quad a_{nm} = 0 \tag{3}$$

$$b_{nm} = \frac{2}{K}\sum_{k=1}^{K} c_n(\theta_k)\sin m\theta_k \quad \text{if} \quad n+m \quad \text{is even, otherwise} \quad b_{nm} = 0 \tag{4}$$

where use was made of the fact that $c_n(\theta_k+\pi) = (-1)^n c_n(\theta_k)$, for an optically thin plasma. The above equations are implemented in the MATLAB environment to readily process the images obtained by the webcams.

3 Setup

A helicon plasma thruster [4] is mounted and centered on the vacuum chamber axis. An aluminium arc is suspended from the chamber ceiling, also centered on the chamber axis. The along-axis positions extends slightly beyond the thruster exit plane such that the plume region can be properly sampled by the webcams. Three aluminium extensions are mounted to the arc, one along the vertical and two are mounted 60 degrees on each side of the vertical as can be seen in figure 2. At the end of each extension a webcam is mounted. The cameras are all, 300 mm from the axis. The alignment of the cameras is done by means of a leveling laser (with $\pm 1^\circ$ accuracy) and verified using a checkerboard. In front of each camera there is a neutral density filter (OD = 1.0) to prevent saturation of the CMOS chip.

4 Results

Here we show some preliminary results obtain while operating with 10 sccm of Argon, 450W of RF power, and a coil current of 20A. Here we only processed the data of the red pixels of the RGB chip as it was found that a large part of the blue pixels was still saturated (it would require thicker filters). Figure 3 shows the cropped image of the center camera with an contour plot overlay of the red pixel intensity. In figure 4 several isosurfaces of the 3D reconstruction of the red pixel intensity can be seen. Figure 5 and 6 show contour plots of the reconstructed axial and transverse cross-section, the later taken at about 3 mm downstream of the exit plane.

5 Conclusion and future work

In the current work only distributions of the red pixel intensity, that is related to the neutral density, have been presented. Neutral density filters of a higher optical density are needed to prevent saturation of the blue

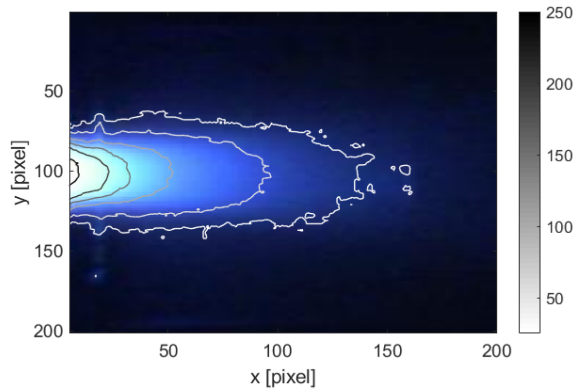

Fig. 3 Top view of thruster plume with red pixel intensity contour plot overlay.

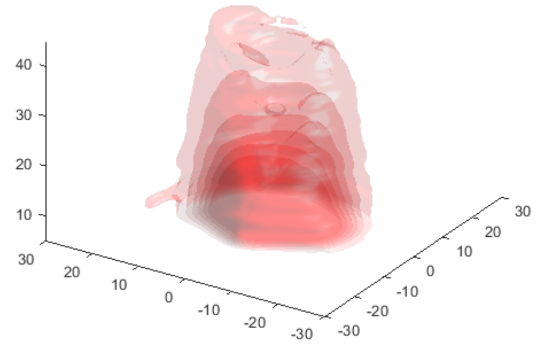

Fig. 4 Iso-surfaces of 3D red pixel intensity distribution.

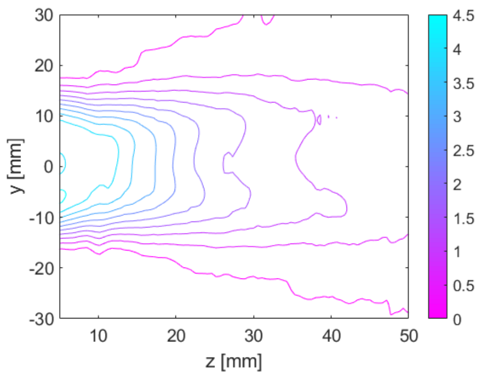

Fig. 5 Axial cross-section of reconstructed red pixel intensity.

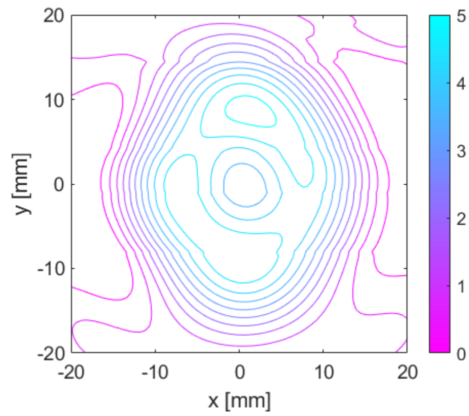

Fig. 6 Transverse cross-section of reconstructed red pixel intensity.

pixels. Data with an significant portion of saturated pixels cannot be trusted as the saturated values can only be considered a lower bound on the actual intensity. Currently only the light intensity is measured. Using different spectral band-pass filters and monochromatic CMOS/CCD chips distributions of single emission lines could be obtain. Using the line-ratio method 3D distributions of the electron temperature could then be obtained. Once the electron temperature is available the plasma density could be derived from an ionic emission line.

Acknowledgments

This work was supported by the Spain's National Research and Development Plan (Project ESP2016-75887). Authors want to thank Carlos Cobos for his support in the manufacturing of the experimental set-up.

References

[1] Hlína J, Chvála J, Šonský J, Gruber J, (2007) Multi-directional optial diagnostics of thermal plasma jets. *Measurement Science and Technology* , vol. 19, pp 015407, doi: 10.1088/0957-0233/19/1/015407

[2] Babou Y, Cannat F, Lequang D, Rond Ch, (2017) Plasma airflow jets diagnosis by means of time-resolved tomography. *Jounarl of Physics: Conference Series* vol 815, pp 012032, doi: 10.1088/1742-6596/815/1/012032

[3] Debnath L, Bhatta D (2008) Integral Transforms and their Application. Chapman and Hall/CRC.

[4] Navarro-Cavallé J, Wijnen M, Fajardo P, Ahedo E, (2018) Experimental characterization of a 1 kW Helicon Plasma Thruster. *Vacuum* vol. 149, pp 69-73, doi: 10.1016/j.vacuum.2017.11.036